Cellular and Molecular Life Sciences (2021) 78:2169–2183
https://doi.org/10.1007/s00018-020-03625-5

Cellular and Molecular Life Sciences

ORIGINAL ARTICLE

Elevated post-ischemic ubiquitination results from suppression of deubiquitinase activity and not proteasome inhibition

Timo Kahles[1,2] · Carrie Poon[1] · Liping Qian[1] · Victoria Palfini[1] · Shanmukha Priya Srinivasan[1] · Shilpa Swaminathan[1] · Ismary Blanco[1] · Reunet Rodney-Sandy[1] · Costantino Iadecola[1] · Ping Zhou[1] · Karin Hochrainer[1]

Received: 21 May 2020 / Revised: 28 July 2020 / Accepted: 18 August 2020 / Published online: 5 September 2020

Abstract

Cerebral ischemia–reperfusion increases intraneuronal levels of ubiquitinated proteins, but the factors driving ubiquitination and whether it results from altered proteostasis remain unclear. To address these questions, we used in vivo and in vitro models of cerebral ischemia–reperfusion, in which hippocampal slices were transiently deprived of oxygen and glucose to simulate ischemia followed by reperfusion, or the middle cerebral artery was temporarily occluded in mice. We found that post-ischemic ubiquitination results from two key steps: restoration of ATP at reperfusion, which allows initiation of protein ubiquitination, and free radical production, which, in the presence of sufficient ATP, increases ubiquitination above pre-ischemic levels. Surprisingly, free radicals did not augment ubiquitination through inhibition of the proteasome as previously believed. Although reduced proteasomal activity was detected after ischemia, this was neither caused by free radicals nor sufficient in magnitude to induce appreciable accumulation of proteasomal target proteins or ubiquitin–proteasome reporters. Instead, we found that ischemia-derived free radicals inhibit deubiquitinases, a class of proteases that cleaves ubiquitin chains from proteins, which was sufficient to elevate ubiquitination after ischemia. Our data provide evidence that free radical-dependent deubiquitinase inactivation rather than proteasomal inhibition drives ubiquitination following ischemia–reperfusion, and as such call for a reevaluation of the mechanisms of post-ischemic ubiquitination, previously attributed to altered proteostasis. Since deubiquitinase inhibition is considered an endogenous neuroprotective mechanism to shield proteins from oxidative damage, modulation of deubiquitinase activity may be of therapeutic value to maintain protein integrity after an ischemic insult.

Keywords Cerebral ischemia–reperfusion · Ubiquitin · Free radical production · Deubiquitinase inhibition

Introduction

Stroke is the second leading cause of death worldwide and a major cause of disability for which therapeutic interventions are very limited [1]. Most strokes result from embolism or thrombosis leading to occlusion of a major cerebral artery (ischemic stroke) [2]. While early reperfusion by intravenous thrombolysis or mechanical thrombectomy ameliorates stroke outcome [3], only a minority of patients can benefit from these interventions due to exclusion criteria, fear of hemorrhagic complications, or, in the case of thrombectomy, lack of specialized resources [4, 5]. Approaches to modulate the cellular and molecular events underlying ischemic cell death would be highly desirable for stroke therapy or as an adjuvant to reperfusion, but a deeper understanding of these events is needed to assess their therapeutic potential [1, 6, 7].

Ubiquitination is an ATP-dependent process that supports cell homeostasis either by promoting protein degradation by the 26S proteasome [8, 9] or by regulating intracellular signaling through non-degradative protein modifications [10, 11]. Cellular stressors, such as reactive oxygen species (ROS), increase protein ubiquitination, which can be either adaptive or maladaptive in nature. On the one hand, reduction in proteasomal activity may result in maladaptive ubiquitination that alters proteostasis and jeopardizes cell survival [12–15]. On the other hand, increased ubiquitination resulting from elevated ubiquitin gene expression

✉ Karin Hochrainer
kah2015@med.cornell.edu

1 Feil Family Brain and Mind Research Institute, Weill Cornell Medicine, New York, NY 10065, USA

2 Department of Neurology, Cantonal Hospital Aarau, 5001 Aarau, Switzerland

[16, 17], activation of ubiquitin conjugases and ligases [18, 19], or reduction in deubiquitinase (DUB) activity [20–22] may promote cell survival by engaging beneficial stress-response pathways [22–24]. It is well established that cerebral ischemia–reperfusion leads to elevation of Triton-insoluble ubiquitinated proteins in neurons, which may represent aggregates or inherently detergent-insoluble proteins [25–28]. However, little is known about the mechanisms driving ubiquitination and its adaptive or maladaptive nature. Identifying the factors involved may provide new insights into post-ischemic protein function and/or degradation, and may create opportunities for the development of new stroke therapies.

Here, we used in vivo and in vitro models of ischemia–reperfusion to investigate the contribution of key determinants of intracellular ubiquitination that are altered by cerebral ischemia: ATP [29], ROS [30, 31], and proteasomal activity [26, 32–35]. We found that recovery of ATP synthesis at reperfusion is essential for initiating post-ischemic ubiquitination, and that, in presence of sufficient ATP, ROS are necessary and sufficient for ubiquitination. Furthermore, contrary to previous belief, the accumulation of ubiquitinated proteins after ischemia was not triggered by failure of proteasomal degradation, but by suppression of DUB activity mediated by ROS. These findings demonstrate for the first time a role of DUB inhibition in post-ischemic ubiquitination, which may represent a protective cell stress response with potential therapeutic implications.

Materials and methods

Mice

All procedures were approved by the Weill Cornell Medicine Institutional Animal Care and Use Committee (IACUC), and were executed according to IACUC, NIH, and ARRIVE guidelines (https://www.nc3rs.org/ARRIVE).

Middle cerebral artery occlusion (MCAO) model of focal ischemia

MCAO was induced using the intraluminal filament model, as previously described [26, 36]. Briefly, 9–10 weeks old C57Bl6/J WT male mice (Jackson Laboratories, Bar Harbor, ME) were anesthetized using isoflurane. A 6–0 nylon blunted monofilament was inserted into the right external carotid artery before it was advanced through the internal carotid artery to obstruct the MCA. The right common carotid artery was simultaneously ligated. The filament was left in place for 40 min (ischemic period), after which it was removed to induce reperfusion. Cerebral blood flow was monitored using a transcranial laser Doppler flowmeter (Periflux System 5010; Perimed Inc, Ardmore, PA), and MCAO was considered successful in animals with > 85% flow reduction during the ischemic period and > 80% increase within the first 10 min of reperfusion. During the procedure, body temperature was maintained at 37 °C. After surgery, mice were placed in clean temperature-controlled cages with free access to food and water. For sham surgery, vessels were visualized and cleared of connective tissue, but no further manipulations were made.

Isolation and culturing of organotypic hippocampal brain slices

Organotypic hippocampal slices were prepared according to the method of Stoppini et al. [37] as previously described [38]. Briefly, hippocampi from 4 to 5 days old C57Bl6/J WT male mice were dissected with sterilized surgical blades in dissection medium [1xHBSS with Ca^{2+}/Mg^{2+}/Phenol Red (Thermo Fisher Scientific, Waltham, MA), 10 mM glucose, 25 mM Hepes pH7.4 (MediaTech Inc, Manassas, VA)] and subsequently cut into 350 µM-thick coronal sections with a McIlwain tissue chopper (Vibratome Company, St. Louis, MO). Slices were transferred onto Millicell CM membrane inserts (0.4 µM pore size, EMD Millipore, Burlington, MA) placed in 6-well plates (Greiner Bio-One, Kremsmuenster, Austria) containing 1 ml culture medium [2 parts MEM (MediaTech Inc), 1 part 1xHBSS, 1 part heat-inactivated horse serum (Atlanta Biologicals, Flowery Branch, GA), 10 mM glucose], and maintained in a humidified chamber flushed with 5% CO_2 at 37 °C. Experiments were carried out on 12–13 days in vitro (DIV).

Oxygen–glucose deprivation (OGD) of hippocampal brain slices and Neuro2a cells

Hippocampal slices were pre-incubated for 30 min in BSS buffer (125 mM NaCl, 5 mM KCl, 1.2 mM Na_2PO_4, 26 mM $NaHCO_3$, 1.8 mM $CaCl_2$, 0.9 mM $MgCl_2$, and 10 mM Hepes pH 7.4) supplemented with 10 mM glucose. Then, slices were placed in deoxygenated BSS buffer without glucose and transferred into an anaerobic chamber (Billups-Rothenberg, San Diego, CA) flushed with 95% N_2 and 5% CO_2. The sealed chamber was incubated at 37 °C for 45–60 min, after which cultures were removed and placed in BSS buffer with glucose for reperfusion for up to 2 h or in culture medium for longer reperfusion times. Control cultures were incubated in BSS in the presence of 10 mM glucose for the duration of the experiment. In certain experiments, reperfusion was either carried out in the presence of oxygen, but without addition of glucose, or in the presence of glucose under anaerobic conditions. To control for viability of slices and efficacy of OGD, a set of slices was assessed by propidium iodide staining (2.5 µg/ml, Sigma-Aldrich, St. Louis, MO) before and 24 h after OGD. Inhibition of E1 activity was achieved through addition of PYR41 (50 µM; Sigma-Aldrich; vehicle 0.2% DMSO) to hippocampal slices at onset of OGD and during reperfusion.

Neuro2a cells (CCL-131) were obtained from the ATCC (Manassas, VA) and grown in DMEM (MediaTech, Manassas, VA) containing 10% FBS (Atlanta Biologicals, Flowery Branch, GA). OGD was performed as described for tissue slices, but for a duration of 5–6 h.

Isolation and detection of Triton-insoluble ubiquitinated and proteasome-target proteins

Organotypic hippocampal slices (six slices pooled/sample) were removed from Millicell inserts with a sterile metal scraper and homogenized with ice-cold homogenization buffer [15 mM Tris–HCl pH 7.6, 250 mM sucrose, 1 mM $MgCl_2$, 2.5 mM EDTA, 1 mM EGTA, 1 mM Na_3VO_4, 5 mM NaF, 20 mM phenylphosphate, 20 mM *N*-ethylmaleimide, 1 mM DTT, and 1 × protease inhibitors (Roche Applied Sciences, Indianapolis, IN)]. Triton X100-resistant proteins were isolated by sequential centrifugation with increasing Triton X100 and KCl concentrations as previously published [26, 39, 40]. Lysates were mixed with SDS-sample buffer (62 mM Tris–HCl pH6.8, 10% glycerol, 2% SDS, bromophenol blue, and 50 mM DTT), loaded on 4–12% gradient SDS-PAGE (Thermo Fisher Scientific) and screened for the absence and presence of high-molecular-weight ubiquitin by Western Blotting with anti-ubiquitin antibody (clone ubi-1, Thermo Fisher Scientific), as well as anti-ubiquitin Lys^{48}-(clone Apu2, EMD Millipore) and Lys^{63}- (clone D7A11, Cell Signaling Technology, Danvers, MA) specific antibodies. GluN1, Shank, and β-actin protein levels were assessed with anti-GluN1 (clone N308/48, BioLegend, San Diego, CA), anti-pan Shank (clone N23B/49, BioLegend), and anti-β-actin (clone AC-15, Sigma-Aldrich) antibodies.

Determination of post-ischemic ATP levels

For ATP measurements, six slices pooled/sample were scraped off the culture insert, dissolved in 2% trichloroacetic acid (TCA), and placed on ice for 30 min. The lysates were made pH neutral by addition of 3vol 0.5 M Tris–acetate pH7.8 and stored at − 80 °C. ATP content in pmol/mg was measured with the Molecular Probes ATP determination kit (Thermo Fisher Scientific) according to the manufacturer's instructions.

Detection of E1 enzyme-ubiquitin thioester bonds

Hippocampal brain slices (six pooled slices/sample) was harvested in thiol-stabilizing buffer [5 mM Tris–HCl pH7.8, 8.7 M urea, 1% Igepal CA-630, 3 mM EDTA, 1 × protease inhibitors (Roche Applied Sciences)], and lysed on ice for 15 min. Samples were sonicated for 10 s and centrifuged at 13 krpm for 15 min at 4 °C. After determination of protein concentrations with the Bio-Rad protein assay (Bio-Rad Laboratories, Hercules, CA), 20 µg total protein solution was mixed with SDS and glycerol to obtain 2.5 and 13% end-concentrations, respectively. Samples were boiled for 5 min and separated under non-reducing conditions on 7% SDS-PAGE followed by Western blotting with anti-Ube1 (clone EPR14204(B), Abcam, Cambridge, UK) antibody. As a control, samples were reduced by addition of 50 mM DTT.

In vitro labeling of E1 enzymes with ubiquitin/DHA

This procedure was essentially performed as developed in [41]. Briefly, hippocampal slices (12 pooled slices/sample) were harvested in ice-cold 50 mM Tris–HCl pH 7.5, 5 mM $MgCl_2$, 250 mM sucrose, 1 mM DTT, 1 × protease inhibitors, by douncing in a glass homogenizer and subsequent sonication for 10 s. Protein concentration in clarified lysates was measured with Bio-Rad protein assay. For E1-ubiquitin/DHA-binding reactions, 25 µg lysates were incubated with 0.5 µg ubiquitin/DHA (UbiQ Bio BV, Amsterdam, The Netherlands) in labeling buffer (50 mM Hepes pH7.5, 100 mM NaCl) in the presence of ATP/$MgCl_2$ (10 mM each at onset of reaction and 1 mM each every 20 min after) with or without 2units apyrase (Sigma-Aldrich) at 37 °C for 1 h. Reactions were stopped by addition of SDS-sample buffer. Samples were resolved on 4–20% gradient SDS-PAGE (Thermo Fisher Scientific), and E1 enzymes and ubiquitin were detected by Western Blotting with anti-Ube1 and anti-ubiquitin antibodies, respectively.

Inhibition, induction, and measurement of ROS production in hippocampal brain slices and Neuro2a cells

The ROS scavengers MnTBAP or 4-hydroxy-Tempo (both Sigma-Aldrich) were added to slice (1 mM) or Neuro2a (250 µM) experiments 30 min prior to OGD, as well as during ischemia and reperfusion. For MnTBAP, vehicle was 100 mM Tris pH8, for 4-hydroxy-Tempo vehicle was ddH_2O. ROS production was induced by addition of hydrogen peroxide (H_2O_2, 1 mM in slices and 500 µM in Neuro2a, Sigma-Aldrich; vehicle ddH2O) or xanthine/xanthine oxidase (X/XO, 600 µM/60 U in slices, EMD Millipore; vehicle 1 mM NaOH) for 60 min. To measure ROS production, slices were incubated with dihydroethidium (DHE) (50 µM, Thermo Fisher Scientific) for 60 min and then monitored in the Texas-Red filter (Ex/Em 518/605 nm) of a Nikon Eclipse TE2000 inverted fluorescence microscope (Nikon, Tokyo, Japan). Images were acquired with a 2 × objective using identical acquisition parameters. Hippocampal CA regions were visually identified, and DHE fluorescence was recorded using IPLab software version 3.9.3 (Scanalytics, Milwaukee, WI) and quantified in Fiji [42].

Measurement of proteasomal catalytic activity with fluorogenic peptides

Tissue slices (six pooled slices/sample) were lysed in ice-chilled buffer containing 20 mM Tris–HCl pH7.5, 1 mM $MgCl_2$, 1 mM EDTA, and 1 mM DTT. Lysates were cleared by centrifugation and protein concentration was measured with the Bio-Rad protein assay. Chymotryptic, tryptic, and caspase-like proteasomal activities were determined in lysates by cleavage of amino-4-methylcoumarin (AMC) from fluorogenic peptide substrates Suc-LLVY-7-AMC, Ac-RLR-AMC, and Z-LLE-AMC (all Boston Biochem, Cambridge, MA), respectively. 20 µg total protein was pre-incubated at 37 °C for 2 min before addition of 10 µM substrate peptides. Thereafter, AMC fluorescence was continuously measured for 1 min at 37 °C using an Ex/Em 380/460 nm filter set on a F-2500 fluorescence spectrophotometer (Hitachi, Tokyo, Japan). AMC fluorescence generated over time was considered directly proportional to proteasomal catalytic activity in samples. Verifying functionality of the assay, addition of 10 µM proteasome inhibitor lactacystin (Boston Biochem) to the reaction completely inhibited generation of AMC fluorescence. Changes in proteasomal activities in slices after ischemia, after induction of ROS production with H_2O_2 or X/XO, or after treatment with the proteasome inhibitor epoxomicin (Boston Biochem) were calculated relative to control conditions.

Assessment of proteasomal activity with UPS reporters in hippocampal brain slices

Hippocampal slices were transduced at DIV 1 with adeno-associated virus 2/1 (AAV2/1) expressing the GFP-based UPS reporter Ub-R-GFP [43] as well as a control mCherry reporter under the neuron-specific Synapsin 1 promoter (AAV2/1-Syn1-Ub-R-GFP-polyA-Syn1-mCherry-WPRE, 0.5 µl, virus titer 1.65×10^{10}/µl, SignaGen Laboratories, Rockville, MD). At DIV12, fluorescence intensities were monitored from the same slice at baseline (control) and after OGD and 6 h reperfusion using a Nikon Eclipse TE2000 microscope equipped with a 2 × objective. Where indicated, 10 µM proteasome inhibitor epoxomicin was added during OGD and reperfusion. Pictures were acquired with a charge-coupled device using identical acquisition parameters. Hippocampal CA regions were visually identified, and GFP relative to mCherry fluorescence was quantified using IPLab software version 3.9.3 (Scanalytics, Milwaukee, WI) and Fiji [42]. Stable detection of mCherry fluorescence was used as indicator for successful viral delivery and slice viability after OGD. Slices in which mCherry fluorescence decreased with OGD/6h reperfusion were omitted from quantification.

Detection of proteasomal activity with UPS reporters in mice

Three-weeks old male C57Bl6/J mice were injected with 6 × 200nL AAV2/1-Syn1-Ub-R-GFP-polyA-Syn1-mCherry-WPRE (virus titer 1.65×10^{10}/µl) or AAV2/1-Syn1-GFPu-polyA-Syn1-mCherry-WPRE ([44], virus titer 1.13×10^{10}/µl, both SignaGen Laboratories) at six different positions. Mice were anesthetized using isoflurane, fixed in a stereotaxic frame, and injected with a Hamilton syringe (10 µl, 33G, Hamilton, Reno, NV) mounted on a micro-injector device (UltraMicroPump, World Precision Instruments, Sarasota, FL). The stereotaxic arm holding the injector was angled at 30° on the right side of the animal. Two burr holes were drilled at 3.5 mm lateral, 0.3 mm caudal from bregma and 4.0 mm lateral, and 0.5 mm rostral to bregma. For each burr hole, injections were performed at 3 depths: + 2.00 mm, + 1.2 mm, and + 0.8 mm from the surface of the cortex. Viral expression was readily detected after 6 weeks, after which MCAO experiments were performed. Where indicated, the proteasome inhibitor Bortezomib (BZ, 50 µg/8 µL, BioVision, Milpitas, CA) or vehicle (25% DMSO) was administered intracerebroventricularly at 2 mm lateral, 0.5 mm caudal to bregma, and a depth of + 2.25 mm. After 16 h reperfusion, animals were transcardially perfused with 4% paraformaldehyde/1 × PBS. Following perfusion, brains were removed and incubated overnight at 4 °C in 4% paraformaldehyde/1 × PBS, and then in 20% sucrose/1 × PBS until they reached equilibration (approximately 24 h). Brains were sectioned using M-1 Embedding Matrix (Thermo Fisher Scientific) on a Leica CM3050S cryostat (Wetzlar, Germany). 30 µm coronal sections were obtained at 200 µm intervals and subsequently stained overnight at 4 °C with Vectashield HardSet antifade mounting medium with DAPI (Vector Laboratories, Burlingame, CA). Images were acquired with a 10 × objective on an Olympus IX83 inverted microscope (Tokyo, Japan) using filter sets for DAPI (Ex/Em 358/461 nm), FITC (Ex/Em 495/519 nm) and Texas-Red (Ex/Em 589/615 nm).

Manipulation and measurement of DUB activity

DUB activity was determined with the fluorogenic peptide ubiquitin-AMC (Boston Biochem). Samples (three pooled slices/sample) were lysed by douncing in 20 mM Tris–HCl pH7.5, 1 mM $MgCl_2$, and 1 mM EDTA, and cleared by centrifugation. 1–5 µg total protein was incubated with 0.5 µM substrate peptide in 200 µl lysis buffer for 1 min at 37 °C and release of AMC from the substrate was measured with a 345/445 nm filter set on a F-2500 fluorescence spectrophotometer (Hitachi, Tokyo, Japan). Addition of 20 mM DUB inhibitor *N*-ethylmaleimide (NEM; Santa Cruz Biotechnology, Dallas, TX) completely inhibited the increase in AMC fluorescence, attesting to the specificity of the assay. Alternatively, DUB activity was measured using the probe Cy5-Ub-PA (UbiQ Bio BV), which covalently links to active DUBs. 25 µg total protein was mixed with 1 µM Cy5-Ub-PA in 25 µl lysis buffer and incubated for 30 min at 37 °C. The reaction was stopped by addition of SDS-sample buffer + 50 mM DTT. Samples were run on 4–12% SDS-PAGE and proteins were transferred onto PVDF membranes (EMD Millipore). Cy5 labeled-protein bands were visualized using the near infra-red 685 nm laser on an Odyssey CLx imager (LI-COR Biosciences, Lincoln, NE). To reduce intracellular DUB activity, Neuro2a cells (20 and 30 µM; 60 min; vehicle 0.1% DMSO) and hippocampal slices (3 mM; 120 min; vehicle 0.6% DMSO) were exposed to the broad-spectrum DUB inhibitor PR-619 [45] (Sigma-Aldrich).

Statistical analysis

Statistical significance between multiple groups was assessed by one-way ANOVA followed by Bonferroni post hoc test. Two group comparisons were analyzed by the two-tailed, unpaired Student's *t* test. *P* values of < 0.05 were considered statistically significant. All analyses were performed using Prism 8 (GraphPad Software, San Diego, CA) and data are presented as mean ± SEM.

Results

Recovery of ATP levels at reperfusion enables ubiquitination after ischemia

Increased post-ischemic ubiquitination is only detected during reperfusion, but not during ischemia [25–27]. First, we sought to determine whether during ischemia ubiquitination comes to a halt because of a lack of ATP, an essential driver of ubiquitination [46]. To this end, we first examined ATP and ubiquitination levels in organotypic hippocampal slices subjected to oxygen–glucose deprivation (OGD), an in vitro model of cerebral ischemia [37, 38]. During OGD, ATP levels significantly dropped correlating with absent ubiquitination (Fig. 1a). After re-establishing oxygen and glucose, to simulate the return of blood flow (reperfusion), ATP levels were partially restored, which was associated with increased ubiquitination (Fig. 1a). If either glucose or oxygen was absent during reperfusion, ATP levels remained low and ubiquitination did not occur (Figs. 1b, c). These data indicate that there is a correlation between ATP levels and ubiquitination during OGD with reperfusion.

To provide further insight into the ATP requirement for ubiquitination after ischemia, we examined binding of ubiquitin to the E1 ubiquitin-activating enzyme, which form an ATP-dependent thioester to initiate protein ubiquitination [46]. Control and OGD-treated slices after 0 and 60 min of reperfusion were harvested under non-reducing conditions to enable detection of the E1 thioester adduct with ubiquitin. The E1–ubiquitin thioester band (E1 + Ub) was readily detected in control slices and after OGD followed by 60 min of reperfusion, but was less abundant without reperfusion (Fig. 1d), when ATP is low and there is no ubiquitination observed (Fig. 1a). The inability of E1 to bind to ubiquitin during OGD was due to lack of ATP, since incubation with recombinant ubiquitin dehydroalanine (Ub-Dha) [41] with excess ATP readily led to the formation of E1 + Ub adducts, which was suppressed by the ATP scavenger apyrase (Fig. 1e). Finally, to confirm that lack of E1 activity can indeed block post-ischemic ubiquitination, we exposed OGD-treated slices to the E1 inhibitor PYR41, which prevents E1 + Ub thioester formation [47]. As expected, PYR41 markedly attenuated ubiquitin accumulation (Fig. 1f). In summary, our data suggest that reperfusion provides the necessary ATP for E1 activation and initiation of post-ischemic ubiquitination.

ROS drive the elevation in post-ischemic ubiquitination

Post-ischemic ubiquitination exceeds pre-ischemic levels [25–27]. Reperfusion initiates the production of ROS [30, 31, 48], which have the potential to raise ubiquitination through several mechanisms [17, 22, 49, 50]. To determine whether ROS augment post-ischemic ubiquitination, we treated slices with ROS scavenger 4-Hydroxy-Tempo and MnTBAP during OGD with reperfusion and monitored ubiquitination levels. Both scavengers suppressed OGD-mediated ROS production, as assessed by DHE fluorescence (Fig. 2a), and blocked ubiquitination (Fig. 2b). Next, we determined whether ROS are sufficient to induce ubiquitination in hippocampal slices, by exposing them to hydrogen peroxide (H_2O_2) or xanthine/xanthine oxidase (X/XO). Both treatments significantly elevated ROS (Fig. 2c, d) and increased ubiquitination as compared to vehicle-treated controls (Fig. 2e, f).

The fate of ubiquitinated proteins is critically dependent on the configuration of the associated ubiquitin. Lys^{48} chains serve mainly as a proteasomal degradation signal [9], while Lys^{63}-linked chains do not [11]. We examined the chain type induced by ROS by treating hippocampal slices with H_2O_2 and X/XO, and probing in Western Blots with ubiquitin linkage-specific antibodies. Exposure to ROS inducers led to enrichment of both Lys^{48} and Lys^{63}-ubiquitin chains (Figs. 3a, b), as previously described

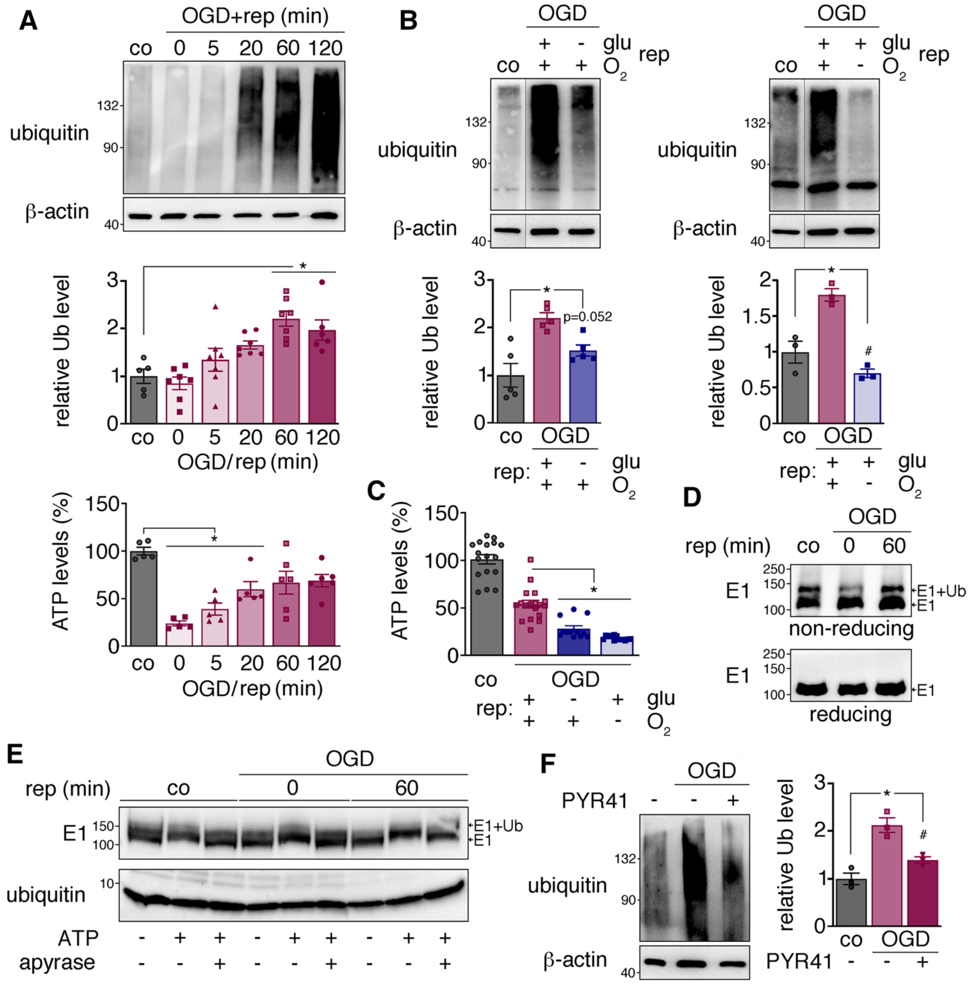

Fig. 1 Post-ischemic ubiquitination is enabled by reperfusion-dependent recovery of ATP production. **a** Hippocampal brain slices were exposed to control condition or OGD for 1 h followed by reperfusion of 0, 5, 20, 60, and 120 min. Tissue slices were harvested, and ubiquitinated proteins were isolated and detected by Western blotting with anti-ubiquitin antibody. β-Actin served as loading control. *$P<0.01$ from co (60 min $P=0.0002$; 120 min $P=0.0044$); $n=5$–7 slice pools/group. ATP concentrations were measured at the same timepoints. *$P<0.01$ from co (0 min $P<0.0001$; 5 min $P=0.0001$; 20 min $P=0.007$); $n=5$–6 slice pools/group. **b** Hippocampal slices underwent OGD, followed by 60 min reperfusion in the presence of oxygen with and without glucose (left panel), or in the presence of glucose with and without oxygen (right panel). Ubiquitin levels were determined as in (a). Left panel: *$P=0.0014$ from co; $P=0.052$ from OGD (+glu); $n=5$ slice pools/group; right panel: *$P=0.0008$ from co; $^{\#}P<0.0001$ from OGD (+O_2); $n=3$ slice pools/group. **c** ATP levels were determined in slices exposed to OGD/60 min reperfusion. *$P<0.001$ from OGD/60 min reperfusion (–glu $P<0.0001$; –O_2 $P<0.0001$); $n=12$ slice pools/group. **d** E1 ubiquitin-activating enzyme binding to ubiquitin was assessed in lysates obtained under non-reducing (upper panel) or reducing (lower panel) conditions from control and OGD samples with and without reperfusion. E1-ubiquitin (E1 + Ub) (upper band) and native E1 (lower band) were visualized by Western blotting with anti-E1 antibody. Blots are representative of three independent experiments. **e** Lysates from control and OGD-treated slices with and without reperfusion were incubated with ubiquitin/DHA in the absence and presence of ATP and the ATP-diphosphohydrolase apyrase. Labeling of E1 enzyme with ubiquitin/DHA was determined by Western Blotting with anti-E1 antibody. Ubiquitin levels were monitored with anti-ubiquitin antibody. The blot is representative of three independent experiments. **f** Ubiquitin accumulation after OGD/60 min reperfusion was examined in the absence and presence of the E1 activating enzyme inhibitor PYR41 by Western Blot and quantified. *$P=0.0016$ from co, $^{\#}P=0.0145$ from OGD-PYR41, $n=3$ slice pools/group. *ATP* adenosine triphosphate, *co* control, *glu* glucose, *min* minutes, *O_2* oxygen, *OGD* oxygen–glucose deprivation, *rep* reperfusion, *Ub* ubiquitin

in ischemia–reperfusion [39, 51]. These data demonstrate that ROS are necessary and sufficient to promote ubiquitination, and that ROS-induced ubiquitination consists of similar ubiquitin chain types than those observed after cerebral ischemia.

Proteasomal impairment does not contribute to elevated post-ischemic ubiquitination

ROS may increase post-ischemic ubiquitination through proteasomal inhibition, which has been reported after focal

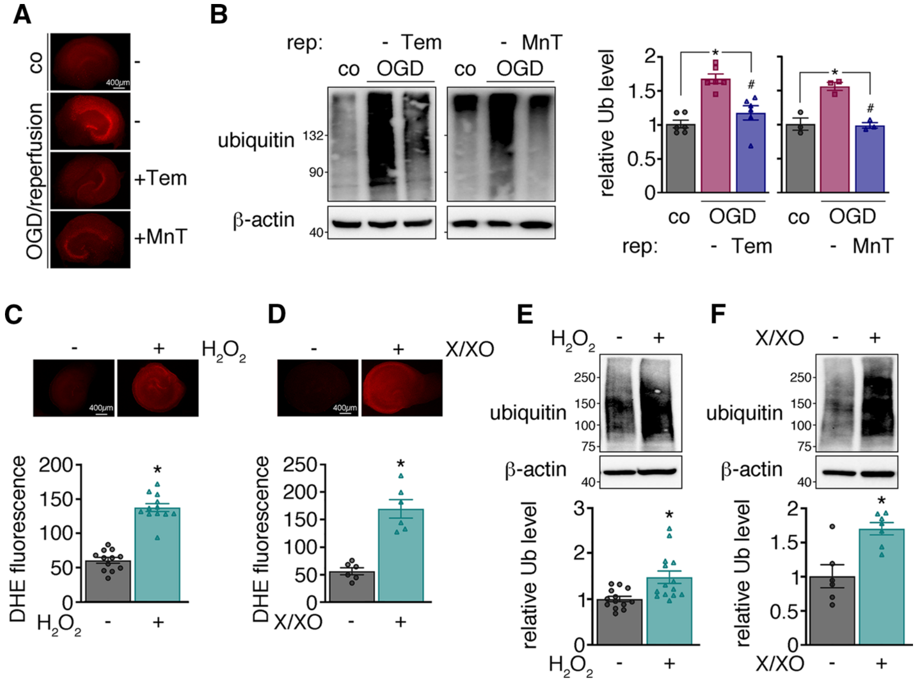

Fig. 2 ROS are necessary and sufficient to promote post-ischemic ubiquitination. **a** Slices were exposed to control conditions or OGD/60 min reperfusion in the absence and presence of the free radical scavengers 4-hydroxy-Tempo or MnTBAP. Free radical production was assessed in CA regions of slices by DHE fluorescence. Representative images are shown. Scale bar = 400 µm. **b** Slices were treated as in **a** and harvested for determination of ubiquitin accumulation. Tem: $^*P<0.0001$ from co; $^{\#}P=0.0013$ from OGD (–Tem); $n=6$/group; MnT: $^*P=0.0032$ from co; $^{\#}P=0.0027$ from OGD (–MnT); $n=3$ slice pools/group. **c** ROS production was induced in hippocampal slices by incubation with H_2O_2 for 1 h. ROS levels were assessed by DHE fluorescence. $^*P<0.0001$, $n=12$ slices/group. Scale bar = 400 µm. **d** Free radical production was initiated by treatment with X/XO for 1 hr and ROS levels were measured by DHE fluorescence. $^*P<0.0001$, $n=6$ slices/group. Scale bar = 400 µm. **e** ROS production was induced as in **c**. Slices were harvested and ubiquitin accumulation in the absence and presence of H_2O_2 was tested by Western Blotting with anti-ubiquitin antibody. β-Actin served as loading control. $^*P=0.0043$, $n=13$–14 slice pools/group. **f** ROS production was induced as in **d** and the level of ubiquitin accumulation was determined. $^*P=0.003$, $n=6$–7 slice pools/group. *co* control, *DHE* dihydroethidium, *H_2O_2* hydrogen peroxide, *MnT* MnTBAP, *O_2* oxygen, *OGD* oxygen–glucose deprivation, *rep* reperfusion, *Tem* 4-hydroxy-Tempo, *Ub* ubiquitin, *X/XO* xanthine/xanthine oxidase

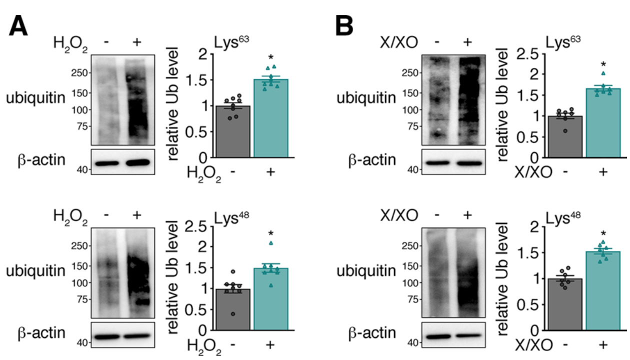

Fig. 3 ROS induce Lys[48] and Lys[63] ubiquitination. **a** Hippocampal slices exposed to H_2O_2 were harvested and lysates were probed for the presence of Lys[63]- and Lys[48]-linked ubiquitin chains. β-Actin served as loading control. Representative blots and quantifications are shown. Lys[63]: $^*P<0.0001$; Lys[48]: $^*P=0.0035$, $n=8$ slice pools/group. **b** Same as in **a**, but treated with X/XO. Lys[63]: $^*P<0.0001$; Lys[48]: $^*P<0.0001$, $n=7$ slice pools/group. *H_2O_2* hydrogen peroxide, *Lys[48]* lysine 48, *Lys[63]* lysine 63, *Ub* ubiquitin, *X/XO* xanthine/xanthine oxidase

cerebral ischemia in mice [26, 32–35]. Therefore, we next sought to determine if reduced catalytic activity of the proteasome plays a role in the post-ischemic accumulation of ubiquitinated proteins. Using a fluorogenic peptide-based assay, we found that OGD in hippocampal slices reduced tryptic, chymotryptic, and caspase-like proteasomal activities by 40–50% (Fig. 4a), a similar magnitude as previously described in mouse stroke models [26, 32–35]. However, lowering proteasomal activity to levels comparable to those observed with OGD using the inhibitor epoxomicin (0.2 µM) [52] did not induce ubiquitin accumulation in hippocampal slices without OGD, whereas further suppression of proteasomal activity with 10 µM epoxomicin did (Fig. 4b, c). Since measurement of proteasome proteolytic capacity using fluorogenic substrates may not accurately reflect the capacity of the proteasome to degrade endogenous proteins, we next determined the levels of two neuronal proteins normally degraded by the proteasome, GluN1, and Shank [53] in OGD with reperfusion. OGD decreased both GluN1 and Shank levels (Fig. 4d), attesting to the fact that proteasomal

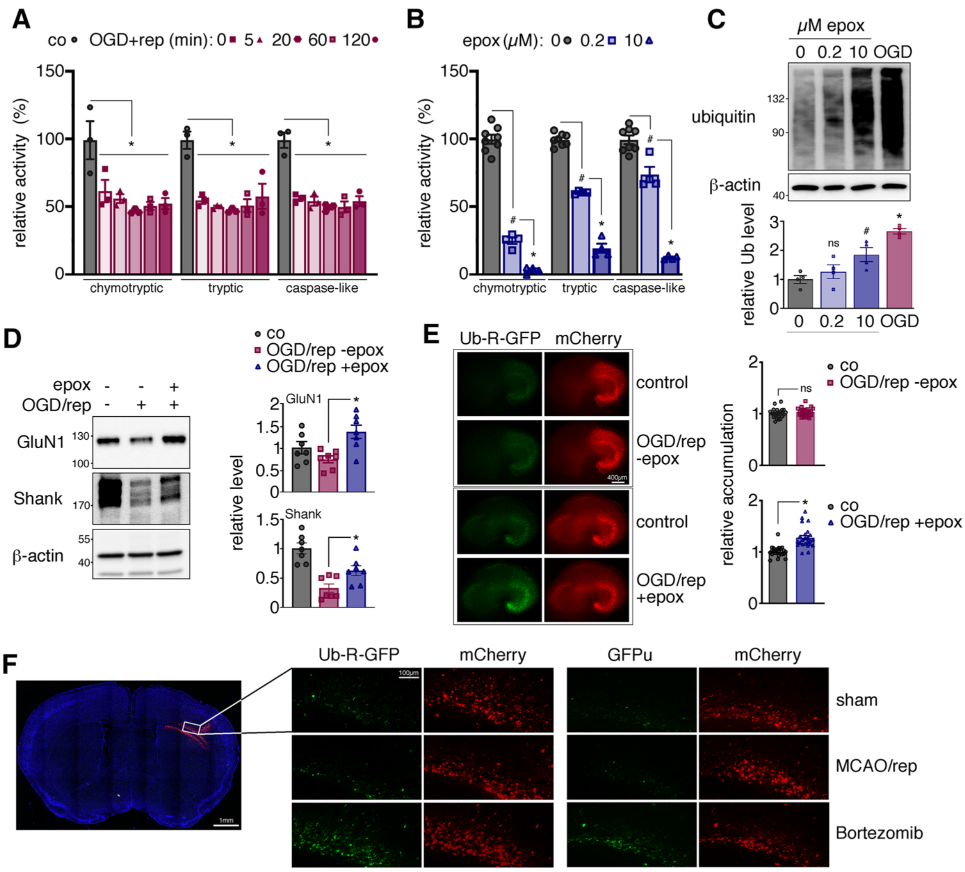

Fig. 4 Proteasome inhibition does not contribute to post-ischemic ubiquitination. **a** Hippocampal slice cultures were exposed to control conditions or 1 h OGD followed by 0, 5, 20, 60, and 120 min reperfusion. Chymotryptic, tryptic, and caspase-like proteasomal activities were determined in lysates by incubation with AMC-labeled fluorogenic peptides carrying respective cleavage sites. The graph shows relative proteasomal activity levels in percent at each time point. Maximal decrease was detected after 20 min reperfusion to 47.2 ± 1.7% (chymotryptic activity), 47.7 ± 1.6% (tryptic activity), and 50.2 ± 2.8% (caspase-like activity) of control. $^*P<0.01$ from co (chymotryptic: 0 min $P=0.0025$, 5 min $P=0.0006$, 20 min $P<0.0001$, 60 min $P=0.0002$, 120 min $P=0.0002$; tryptic: 0 min $P=0.0002$, 5 min $P<0.0001$, 20 min $P<0.0001$, 60 min $P<0.0001$, 120 min $P=0.0005$; caspase-like: 0 min $P=0.0006$, 5 min $P=0.0004$, 20 min $P=0.0001$, 60 min $P=0.0001$, 120 min $P=0.0004$); $n=3$ slice pools/group. **b** Slices were treated with the proteasomal inhibitor epoxomicin at 0.2 and 10 µM for 2 h, and proteasomal activities were measured as in (A). Chymotryptic: $^{\#}P<0.0001$; tryptic: $^{\#}P<0.0001$; caspase-like: $^{\#}P=0.0006$ from untreated; chymotryptic: $^*P=0.0021$; tryptic: $^*P<0.0001$; caspase-like $^*P<0.0001$ from 0.2 µM; $n=4$ slice pools/group. **c** Ubiquitin accumulation was assessed in slices treated with epoxomicin for 2h and compared to OGD/60 min reperfusion by Western Blotting. Optical densities of ubiquitin-stained bands were measured and changes in ubiquitin levels were expressed relative to untreated controls. β-Actin served as normalization and loading control. $^{\#}P=0.018$ and $^*P<0.0001$ from untreated; $n=4$ slice pools/group. **d** Protein levels of neuronal proteasomal targets GluN1 and Shank were determined before and after OGD with and without addition of 10 µM epoxomicin, and quantified relative to β-actin. GluN1: $^*P=0.0016$; Shank: $^*P=0.018$ from OGD/rep –epox; $n=7$ slice pools/group. **e** Hippocampal slices were transduced with AAV2/1 expressing the UPS reporter Ub-R-GFP and a control reporter mCherry, both under the neuronal SYN1 promoter. Green and red fluorescence was monitored in control and OGD-treated slices after 6 h reperfusion. As positive control, after OGD the proteasome was inhibited with epoxomicin (10 µM). Ub-R-GFP levels relative to mCherry were quantified in the CA region. $^*P<0.0001$; $n=24$ slices/group. Scale bar = 400 µm. **f** Mice were intracortically injected with neuronal AAV2/1 expressing Ub-R-GFP or GFPu together with mCherry. The targeted expression area is shown in a representative DAPI-stained coronal brain section, with a scale bar of 1 mm. Mice underwent sham or MCAO surgery followed by 16 h reperfusion. Intracerebroventricular injection with 50 µg Bortezomib was performed to show maximal possible accumulation of UPS reporters. Fluorescence levels of reporters were monitored and representative images are shown. Scale bar = 100 µm. Ub-R-GFP $n=3$ mice/group. GFPu $n=2$–3 mice/group. *co* control, *epox* epoxomicin, *h* hours, *min* minutes, *ns* not significant, *OGD* oxygen–glucose deprivation, *rep* reperfusion, *Ub* ubiquitin

degradation was not compromised by OGD. In contrast, degradation of both proteins was blocked if proteasomal activity was inhibited by > 80% with epoxomicin (Fig. 4d). To provide further evidence that proteasomal degradation is preserved after ischemia we used the neuronally expressed ubiquitin–proteasome (UPS) reporters Ub-R-GFP [43] and GFPu [44]. Consistent with the above data, Ub-R-GFP levels remained unaffected by OGD alone and were only increased by > 80% proteasome inhibition (Fig. 4e). To assess UPS reporter levels after ischemia in mice, we performed transient middle cerebral artery occlusion (MCAO) after intracortical injection of AAV-driven reporters. In agreement with OGD, Ub-R-GFP fluorescence did not increase in cortical neurons after transient focal ischemia, but it readily accumulated after inhibition of the proteasome with Bortezomib in naïve mice (Fig. 4f, left panels). Similar results were obtained with another UPS reporter, GFPu (Fig. 4f, right panels). Therefore, post-ischemic proteasomal inhibition is not sufficient to induce accumulation of ubiquitinated proteins.

ROS can deactivate proteasomal subunits [15, 50, 54–56]. Therefore, we sought to investigate if ROS play a role in post-ischemic proteasomal inhibition (Fig. 4a). OGD induced inhibition of proteasomal activity even in the absence of reperfusion (Fig. 5a) or in absence of oxygen at reperfusion (Fig. 5b) conditions in which ROS are not generated (Fig. 5c, d). In addition, proteasomal activity was not affected by treating the slices with the ROS generators H_2O_2 and X/XO (Fig. 5e, f). Therefore, ROS production does not contribute to post-ischemic proteasomal inhibition.

ROS increase post-ischemic protein ubiquitination by suppressing deubiquitinase activity

The data presented above demonstrate that ROS do not trigger post-ischemic ubiquitination through the proteasome, implicating other mechanisms. In yeast, elevated ROS production promotes Lys^{48} and Lys^{63} ubiquitination by inhibiting DUBs [22]. Therefore, we tested the hypothesis that decreased DUB activity contributes to ROS-dependent post-ischemic protein ubiquitination. First, we assessed DUB activity levels in H_2O_2-treated Neuro2a cells, which, like hippocampal slices (Fig. 2d), showed increased ubiquitination in the presence of free radicals (Fig. 6a). We assayed DUB activity using the DUB activation probes ubiquitin-AMC and ubiquitin-PA [57]. H_2O_2 treatment of Neuro2a cells led to a 31 ± 5% decreased cleavage of ubiquitin-AMC (Fig. 6b) as well as a 27 ± 2% reduction in binding of ubiquitin-PA to DUBs (Fig. 6c), indicating that ROS production lowered DUB activity in these cells. Next, we asked whether OGD, like H_2O_2, inhibits DUB activity. Neuro2a cells exposed to OGD exhibited increased ubiquitination (Fig. 6d), which was associated with a 26 ± 6% decreased DUB activity, measured by ubiquitin-AMC cleavage (Fig. 6e), and a 31 ± 3% decrease, assessed by the binding of ubiquitin-PA to DUBs (Fig. 6f). The reduction in DUB activity was caused by free radicals, since scavenging ROS by MnTBAP restored DUB activity after OGD (Fig. 6g). A reduction in DUB activity similar to Neuro2a cells was also observed in hippocampal slices exposed to H_2O_2 (20 ± 2%; Fig. 6h) or OGD (17 ± 2%; Fig. 6i), indicating that this

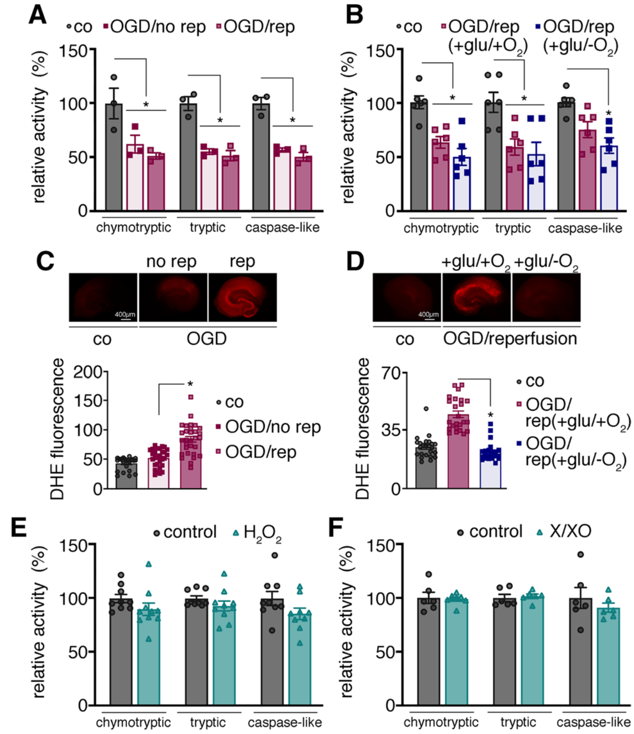

Fig. 5 ROS promote ubiquitination without causing proteasomal inhibition. **a** Proteasomal chymotryptic, tryptic, and caspase-like activities were measured using fluorogenic substrate peptides in slices exposed to control or OGD with or without reperfusion. $*P < 0.001$ from co (chymotryptic: OGD + rep $P < 0.0001$; OGD − rep $P = 0.001$; tryptic: OGD + rep $P < 0.0001$; OGD-rep $P = 0.0001$; caspase-like: OGD + rep $P < 0.0001$; OGD-rep $P = 0.0003$); $n = 3$ slice pools/group. **b** Proteasomal activities were measured and quantified as in **a** in slices maintained under control conditions or OGD followed by reperfusion in presence and absence of oxygen. $*P < 0.05$ from co (chymotryptic: OGD/re $P + O_2$ $P = 0.0021$; OGD/rep − O_2 $P < 0.0001$; tryptic: OGD/re $P + O_2$ $P = 0.0006$; OGD/rep − O_2 $P < 0.0001$; caspase-like: OGD/re $P + O_2$ $P = 0.042$; OGD/rep − O_2 $P = 0.0009$); $n = 6$ slice pools/group. **c** ROS production was assessed by DHE fluorescence in CA regions of hippocampal slices treated as in **a**. Representative images as well as quantification of $n = 24$–30 slices/group are shown. $*P < 0.0001$ from OGD-rep. Scale bar = 400 µm. **d** Free radical production was determined by DHE fluorescence in slices treated as in **b**. $*P < 0.0001$ from OGD/re $P + O_2$; $n = 24$ slices/group. Representative images and quantification are shown. Scale bar = 400 µm. **e** ROS production was induced in hippocampal slices by incubation with H_2O_2 for 1 h, after which proteasomal activities were measured. $n = 9$–10 slice pools/group. **f** Free radical production was initiated by treatment with X/XO and proteasomal activities were measured. $n = 6$–7 slice pools/group. *co* control, *DHE* dihydroethidium, *H_2O_2* hydrogen peroxide, *O_2* oxygen, *OGD* oxygen–glucose deprivation, *rep* reperfusion, *X/XO* xanthine/xanthine oxidase

phenomenon is not only present in the cell line. Therefore, ROS produced by H_2O_2 or OGD reduce DUB activity by approx. 20–30%.

To test whether the decrease in DUB activity observed after OGD is sufficient to increase ubiquitination, we treated Neuro2a cells and hippocampal slices with the DUB

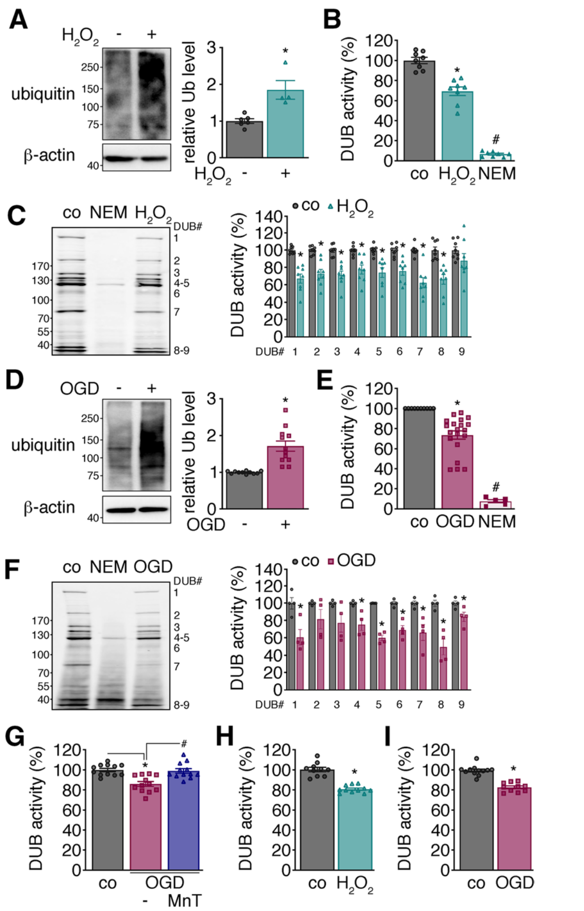

Fig. 6 ROS production induced by H_2O_2 or OGD reduces intracellular DUB activity. **a** Neuro2a cells were treated for 60 min with 500 µM H_2O_2 and harvested for measuring ubiquitination levels. A representative blot and quantification are shown. $^*P=0.0043$, $n=4$–6/group. **b** Cells were treated as in **a** and DUB activity was measured by incubating lysates with a fluorogenic ubiquitin molecule coupled to AMC. Addition of the DUB inhibitor NEM showed maximal achievable inhibition. $^*P<0.0001$, $^\#P<0.0001$ from control; $n=8$/group. **c** Experiment was performed as in **b**. Lysates were incubated with the DUB activity probe ubiquitin-PA coupled to Cy5. Binding of DUBs to the probe was examined after SDS-PAGE by direct detection of Cy5 fluorescence on PVDF membranes. Band intensities, which are directly proportional to the activities of nine unidentified DUBs (#1–9), were quantified. DUB1 $^*P<0.0001$, DUB2 $^*P=0.0002$, DUB3 $^*P<0.0001$, DUB4 $^*P=0.0014$, DUB5 $^*P=0.0007$, DUB6 $^*P=0.0005$, DUB7 $^*P<0.0001$, DUB8 $^*P=0.0002$; $n=8$/group. **d** Neuro2a cells were exposed to OGD/30 min reperfusion and harvested to determine ubiquitination levels. A representative blot and quantification are shown. $^*P<0.0001$, $n=11$–12/group. **e** Cells were treated as in **d** to measure DUB activity using ubiquitin-AMC as substrate. $^*P<0.0001$, $^\#P<0.0001$ from control; $n=5$–10/group. **f** DUB activity was analyzed as in **c** using ubiquitin-PA coupled to Cy5. DUB1 $^*P=0.012$, DUB4 $^*P=0.011$, DUB5 $^*P<0.0001$, DUB6 $^*P=0.0014$, DUB7 $^*P=0.012$, DUB8 $^*P=0.002$, DUB9 $^*P=0.042$; $n=4$/group. **g** Neuro2a cells were exposed to OGD/reperfusion in the absence and presence of the free radical scavenger MnTBAP, and DUB activity was measured with ubiquitin-AMC. $^*P=0.0002$ from control, $^\#P=0.0004$ from OGD (–MnT); $n=12$/group. **h** Hippocampal slices exposed to H_2O_2 were harvested and lysates were probed for DUB activity with ubiquitin-AMC. $^*P<0.0001$, $n=10$–11 slice pools/group. **i** Hippocampal slices exposed to OGD/reperfusion were harvested and lysates were probed for DUB activity with ubiquitin-AMC. $^*P<0.0001$, $n=10$–12 slice pools/group. *co* control, *DUB* deubiquitinase, *H_2O_2* hydrogen peroxide, *MnT* MnTBAP, *NEM* N-ethylmaleimide, *OGD* oxygen glucose deprivation, *Ub* ubiquitin

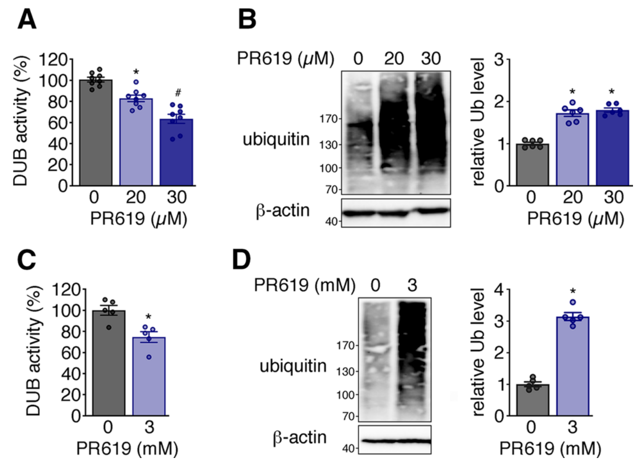

Fig. 7 The OGD-mediated decrease in DUB activity is sufficient to induce ubiquitination. **a** Neuro2a cells were treated for 60 min with 0, 20, and 30 µM broad-spectrum DUB inhibitor PR619, and DUB activity was measured by incubating lysates with a fluorogenic ubiquitin molecule coupled to AMC. $^*P=0.0022$, $^\#P<0.0001$ from 0 µM PR619; $n=8$/group. **b** Cells were treated as in **a** and harvested for measuring ubiquitination levels. A representative blot and quantification are shown. $^*P<0.0001$, $n=6$/group. **c** Hippocampal brain slices were exposed to 3 mM PR619 for 2 h. DUB activity was determined as in **a**. $^*P=0.0062$ from 0 µM PR619; $n=5$ slice pools/group. **d** PR619-treated brain slices were harvested and analyzed for induction of ubiquitination by Western Blotting. $^*P<0.0001$, $n=5$ slice pools/group. *DUB* deubiquitinase, *Ub* ubiquitin

inhibitor PR-619 at concentrations that lowered DUB activity by 20–30%. PR-619 reduced DUB activity in Neuro2a cells by 18 ± 4% at 20 µM and 37 ± 5% at 30 µM, (Fig. 7a), both of which induced ubiquitination (Fig. 7b). Similarly, PR-619 decreased DUB activity in brain slices by 25 ± 7% (Fig. 7c), which significantly elevated ubiquitination (Fig. 7d). These data indicate that the degree of DUB inhibition induced by OGD is sufficient to increase post-ischemic protein ubiquitination.

Discussion

In this study, we investigated mechanisms underlying elevated post-ischemic ubiquitination. Our first new finding is that the absence of ubiquitination during the ischemic period and its initiation at reperfusion is dictated by ATP availability. ATP is required for activation of E1 enzymes to initiate the enzymatic cascade leading to ubiquitination of target proteins [46]. We provided evidence that during ischemia, ATP levels drop below the threshold that is necessary for activating E1, which answers the long-standing question of why ubiquitination is not observed in ischemia without reperfusion or in brain regions in which reperfusion is limited [26], conditions in which ATP is severely depleted [58, 59]. In addition, this finding suggests that ubiquitination specifically occurs in cells with survival potential, in which ATP synthesis is restored. Second, we found that, in the presence of enough ATP, ROS are necessary and sufficient to boost ubiquitination after ischemia above physiological levels. Third, and most importantly, we provided evidence that ROS trigger ubiquitination by dampening intracellular DUB activity and not by inhibiting the proteasome as previously believed. On these bases, our work introduces a novel pathway involved in post-ischemic ubiquitination and may initiate a paradigm shift in our understanding of the role of ubiquitination in ischemia.

ROS can augment ubiquitination by different molecular mechanisms, including inhibition of the proteasome, the main cellular machinery for degradation of ubiquitinated proteins [15, 50, 54–56]. In fact, elevated post-ischemic ubiquitination has been traditionally attributed to proteasome inhibition [26, 32–35]. We did find that proteasomal activity is reduced post-ischemia, but this was not associated with deficient protein degradation. A possible reason for this finding might be that a greater than 80% inhibition is needed for accumulation of ubiquitinated proteins [43], whereas ischemia–reperfusion lowers proteasomal activity by only 40–50% (Fig. 4a, [26, 32–35]). Another explanation could be that measuring proteasome activity by cleavage capacity against fluorogenic peptides in vitro, as done in Fig. 4a and previous studies [26, 32–35], does not adequately reflect endogenous proteasomal function [60]. Proteasomes are multi-subunit complexes that tend to disintegrate when isolated, which may influence in vitro measures [60]. Also, proteasomes exist as different composites, 26S and 20S, which have different specificities for degradation of ubiquitinated vs. non-ubiquitinated, often oxidized, proteins [61], which cannot be distinguished by fluorogenic peptides [60]. To avoid these caveats, in the present study, we measured the ability of proteasomes to degrade endogenous ubiquitinated substrates, such as ubiquitin–proteasome reporters and the endogenous neuronal proteasome targets GluN1 and Shank, which we found not to be impaired. In addition, ROS were not causally associated with the decrease in proteasome activity measured after ischemia. First, we have shown that proteasomal inhibition occurs during ischemia before onset of ROS production and, as such, ROS cannot be responsible for triggering the inhibition. Second, we found that reduction in proteasome activity during reperfusion takes place even when ROS are absent. Third, oxidative stress in the ischemic mouse brain persists even after recovery of proteasomal activity [26, 33, 35]. This suggests that mechanisms independent of the proteasome must lead to the increase in ubiquitination induced by ROS. Proteasomal inhibition during ischemia–reperfusion could be the result of separation of 19S and 20S proteasomal subunits, which has been described in global ischemia models [32, 35, 62], but, as shown here, such inhibition is not sufficient to prevent protein degradation. In addition to the proteasome, degradation of ubiquitinated proteins may be controlled by autophagy, and hence, accumulation could result from autophagy deficiency. However, this possibility seems unlikely, because (a) autophagy is not affected until later in reperfusion [63–66], when the increase in ubiquitination has already occurred, and (b) autophagy has been shown to be up-regulated after ischemia [63, 65, 66], which would enhance rather than suppress protein clearance.

Apart from the proteasome, ROS were shown to induce ubiquitination through increased expression of ubiquitin or proteins involved in ubiquitin conjugation [16, 18, 19, 67, 68]. However, given that the induction of ubiquitination after ischemia is very rapid (Fig. 1a and [26]) and that ischemia suppresses protein synthesis [69–71], regulation of post-ischemic ubiquitination through translational events seems rather unlikely. Instead, it is more plausible that ROS trigger post-ischemic changes in UPS enzyme activities. ROS can exacerbate ubiquitination by over-activation of the E1 enzyme [17], which, as discussed above, we found not to be the case after ischemia. ROS can also inactivate DUBs [20, 21, 72], and we found that this mechanism was the main driver of increased post-ischemic ubiquitination. Post-ischemic DUB inhibition is reversed by the superoxide dismutase mimetic MnTBAP, suggesting ROS, but also reactive nitrogen species (RNS) as potential responsible modifier resulting in DUB suppression. Since most DUBs are inhibited in the presence of ROS [20, 21], whereas only one DUB, UCH-L1, has been identified as RNS target [73, 74], DUB inhibition through ROS rather than RNS appears more likely after ischemia. Mammalian cells contain about 90–100 DUB enzymes, 90% of which are cysteine- and 10% metalloproteases [75]. Cysteine DUBs are generally susceptible to inactivation by ROS, while metalloproteases appear resistant [20, 21, 72]. A previous study found that among cysteine DUBs, about 40% were not responsive to redox-regulation [21], which could partly explain the overall moderate inhibition level that we obtained after ischemia. In addition to DUB inhibition, increased ubiquitination could also be associated with augmented E2 conjugase or E3 ligase activities. It is currently not known whether E2 or E3 enzymatic activities are altered with ischemia. Protein levels of E3 ligases Nedd4-2 and Itch are up-regulated after ischemia [76], but if this is connected with increased activity is elusive. With regards to ROS, catalytic cysteines of E2 enzymes do not appear to be susceptible to oxidation [77] and regulation of E3 catalytic sites by ROS has not been described so far.

There is evidence that ubiquitination and DUB inhibition contribute to oxidative stress resistance. For example, deletion of the Ubc gene increases susceptibility to H_2O_2 exposure in yeast [78] and arsenite-induced ROS in mammalian cells [79]. In addition, H_2O_2 exposure in yeast inhibits the DUB Ubp2 leading to enrichment of ubiquitinated ribosomal proteins that promote cell survival [22]. DUB inhibition in H_2O_2-treated mammalian cells facilitates PCNA ubiquitination to induce a DNA damage tolerance program [21]. Therefore, the ROS-dependent elevation in post-ischemic ubiquitination could be part of an endogenous adaptive response. To further investigate this, specific DUBs whose ROS-dependent modification affects post-ischemic ubiquitination need to be identified. Altered activity of two DUBs, UCH-L1 and USP14, has been reported to impact ischemic injury. While inhibition of USP14 is neuroprotective in mice undergoing focal ischemia [80], inactivation of UCH-L1 aggravates neuronal injury after hypoxia–ischemia [81, 82]. USP14 activity is not regulated by its redox state [21], whereas UCH-L1 is inactivated by ROS, at least in vitro [20, 21].

Another line of evidence suggesting that post-ischemic ubiquitination could be an adaptive response to cell stress relates to the nature of the ubiquitination process. Ubiquitin is attached to target proteins as monomer or as chains linked via different positions in ubiquitin, achieving different outcomes [11]. Lys^{48}-linked chains mainly target proteins for degradation by the proteasome, whereas Lys^{63}-linked chains non-proteolytically regulate cell signaling events [11, 28]. The ability of ubiquitination to protect cells against stress is particularly dependent on conjugation of Lys^{63}-linked ubiquitin chains [22, 23]. Lys^{63}-linked ubiquitin chains are also prominently found after ischemia [39, 51], and, as shown here, could be generated through ROS. ROS and ischemia also produce Lys^{48}-linked chains [39, 51], without affecting the proteasome, likely by inhibiting Lys^{48}-specific DUBs. Although limited, there is some evidence that Lys^{48}-linked ubiquitin can perform non-proteolytic functions [83, 84]. Identification of Lys^{48}- and Lys^{63}-ubiquitin targets will aid in elucidating respective consequences and will, therefore, be subject of future investigations.

In summary, our study demonstrates that post-ischemic ubiquitination occurs independently of the proteasome and is mediated by ROS-dependent DUB inhibition. Although the implications for cerebral ischemic injury remain to be defined, the abundance of non-degradative Lys^{63}-ubiquitin chains associated with DUB inhibition supports an adaptive role of post-ischemic ubiquitination in cell stress defense. Therefore, as shown in some other disease models, DUB inhibition may provide an endogenous cytoprotective mechanism against oxidative stress and ischemic brain injury which, if better understood, may provide clues to novel treatments for ischemic stroke.

Acknowledgements The authors wish to thank Diego Santisteban Vargas for technical assistance with ubiquitin-AMC experiments.

Author contributions TK, LQ, PZ, and KH conducted brain slice and neuron experiments and performed data analysis; CP, VP, and KH performed MCAO experiments, associated histology and data analysis; SPS contributed to DUB activity experiments; SS aided with proteasome experiments; IB, VP, RRS, and SPS contributed to Western blotting experiments; PZ, CI, and KH provided funding; KH and CI supervised the research and wrote the manuscript.

Funding This study was supported by National Institute of Health (NIH) grants R01-NS109588 to KH, R01-NS34179 to CI, and R01-NS067078 to PZ, as well as a post-doctoral research grant from the Deutsche Forschungsgemeinschaft (KA2279/4-1) to TK. KH is the Finbar and Marianne Kenny Research Scholar in Neurology at Weill Cornell Medicine. Support from the Feil Family Foundation is gratefully acknowledged.

Availability of data and materials All data needed to evaluate the conclusions in the paper are present in the manuscript.

Compliance with ethical standards

Conflict of interest CI is on the Scientific Advisory Board of Broadview Ventures. The other authors declare that they have no competing interests.

Ethics approval All procedures involving mice were approved by the Weill Cornell Medicine Institutional Animal Care and Use Committee (IACUC) and were executed according to IACUC, NIH, and ARRIVE guidelines (https://www.nc3rs.org/ARRIVE).

Consent for publication All authors consent to this submission.

References

1. Benjamin EJ, Muntner P, Alonso A, Bittencourt MS, Callaway CW, Carson AP, Chamberlain AM, Chang AR, Cheng S, Das SR, Delling FN, Djousse L, Elkind MSV, Ferguson JF, Fornage M, Jordan LC, Khan SS, Kissela BM, Knutson KL, Kwan TW, Lackland DT, Lewis TT, Lichtman JH, Longenecker CT, Loop MS, Lutsey PL, Martin SS, Matsushita K, Moran AE, Mussolino ME, O'Flaherty M, Pandey A, Perak AM, Rosamond WD, Roth GA, Sampson UKA, Satou GM, Schroeder EB, Shah SH, Spartano NL, Stokes A, Tirschwell DL, Tsao CW, Turakhia MP, VanWagner LB, Wilkins JT, Wong SS, Virani SS, American Heart Association Council on E, Prevention Statistics C, Stroke Statistics S (2019) Heart Disease and Stroke Statistics-2019 update: a report from the American Heart Association. Circulation 139(10):e56–e528. https://doi.org/10.1161/CIR.0000000000000659
2. Campbell BCV, De Silva DA, Macleod MR, Coutts SB, Schwamm LH, Davis SM, Donnan GA (2019) Ischaemic stroke. Nat Rev Dis Primers 5(1):70. https://doi.org/10.1038/s41572-019-0118-8
3. Mendez AA, Samaniego EA, Sheth SA, Dandapat S, Hasan DM, Limaye KS, Hindman BJ, Derdeyn CP, Ortega-Gutierrez S (2018) Update in the early management and reperfusion strategies of patients with acute ischemic stroke. Crit Care Res Pract 2018:9168731. https://doi.org/10.1155/2018/9168731
4. Tawil SE, Cheripelli B, Huang X, Moreton F, Kalladka D, MacDougal NJ, McVerry F, Muir KW (2016) How many stroke patients might be eligible for mechanical thrombectomy? Eur Stroke J 1(4):264–271. https://doi.org/10.1177/2396987316667176

5. Rinaldo L, Rabinstein AA, Cloft H, Knudsen JM, Castilla LR, Brinjikji W (2019) Racial and ethnic disparities in the utilization of thrombectomy for acute stroke. Stroke 50(9):2428–2432. https://doi.org/10.1161/STROKEAHA.118.024651
6. Bosetti F, Koenig JI, Ayata C, Back SA, Becker K, Broderick JP, Carmichael ST, Cho S, Cipolla MJ, Corbett D, Corriveau RA, Cramer SC, Ferguson AR, Finklestein SP, Ford BD, Furie KL, Hemmen TM, Iadecola C, Jakeman LB, Janis S, Jauch EC, Johnston KC, Kochanek PM, Kohn H, Lo EH, Lyden PD, Mallard C, McCullough LD, McGavern LM, Meschia JF, Moy CS, Perez-Pinzon MA, Ramadan I, Savitz SI, Schwamm LH, Steinberg GK, Stenzel-Poore MP, Tymianski M, Warach S, Wechsler LR, Zhang JH, Koroshetz W (2017) Translational stroke research: vision and opportunities. Stroke 48(9):2632–2637. https://doi.org/10.1161/STROKEAHA.117.017112
7. Chamorro A, Dirnagl U, Urra X, Planas AM (2016) Neuroprotection in acute stroke: targeting excitotoxicity, oxidative and nitrosative stress, and inflammation. Lancet Neurol 15(8):869–881. https://doi.org/10.1016/S1474-4422(16)00114-9
8. Hershko A, Eytan E, Ciechanover A, Haas AL (1982) Immunochemical analysis of the turnover of ubiquitin-protein conjugates in intact cells. Relationship to the breakdown of abnormal proteins. J Biol Chem 257(23):13964–13970
9. Johnson ES, Ma PC, Ota IM, Varshavsky A (1995) A proteolytic pathway that recognizes ubiquitin as a degradation signal. J Biol Chem 270(29):17442–17456
10. Chen ZJ, Sun LJ (2009) Nonproteolytic functions of ubiquitin in cell signaling. Mol Cell 33(3):275–286
11. Komander D, Rape M (2012) The ubiquitin code. Annu Rev Biochem 81:203–229. https://doi.org/10.1146/annurev-biochem-060310-170328
12. Menendez-Benito V, Verhoef LG, Masucci MG, Dantuma NP (2005) Endoplasmic reticulum stress compromises the ubiquitin-proteasome system. Hum Mol Genet 14(19):2787–2799. https://doi.org/10.1093/hmg/ddi312
13. Salomons FA, Menendez-Benito V, Bottcher C, McCray BA, Taylor JP, Dantuma NP (2009) Selective accumulation of aggregation-prone proteasome substrates in response to proteotoxic stress. Mol Cell Biol 29(7):1774–1785. https://doi.org/10.1128/MCB.01485-08
14. Goldberg AL (2003) Protein degradation and protection against misfolded or damaged proteins. Nature 426(6968):895–899
15. Wang X, Yen J, Kaiser P, Huang L (2010) Regulation of the 26S proteasome complex during oxidative stress. Sci Signal 3(151):ra88. https://doi.org/10.1126/scisignal.2001232
16. Fornace AJ Jr, Alamo I Jr, Hollander MC, Lamoreaux E (1989) Ubiquitin mRNA is a major stress-induced transcript in mammalian cells. Nucleic Acids Res 17(3):1215–1230
17. Shang F, Gong X, Taylor A (1997) Activity of ubiquitin-dependent pathway in response to oxidative stress. Ubiquitin-activating enzyme is transiently up-regulated. J Biol Chem 272(37):23086–23093
18. Seufert W, Jentsch S (1990) Ubiquitin-conjugating enzymes UBC4 and UBC5 mediate selective degradation of short-lived and abnormal proteins. EMBO J 9(2):543–550
19. Qian SB, McDonough H, Boellmann F, Cyr DM, Patterson C (2006) CHIP-mediated stress recovery by sequential ubiquitination of substrates and Hsp70. Nature 440(7083):551–555. https://doi.org/10.1038/nature04600
20. Cotto-Rios XM, Bekes M, Chapman J, Ueberheide B, Huang TT (2012) Deubiquitinases as a signaling target of oxidative stress. Cell Rep 2(6):1475–1484. https://doi.org/10.1016/j.celrep.2012.11.011
21. Lee JG, Baek K, Soetandyo N, Ye Y (2013) Reversible inactivation of deubiquitinases by reactive oxygen species in vitro and in cells. Nat Commun 4:1568. https://doi.org/10.1038/ncomms2532
22. Silva GM, Finley D, Vogel C (2015) K63 polyubiquitination is a new modulator of the oxidative stress response. Nat Struct Mol Biol 22(2):116–123. https://doi.org/10.1038/nsmb.2955
23. Arnason T, Ellison MJ (1994) Stress resistance in *Saccharomyces cerevisiae* is strongly correlated with assembly of a novel type of multiubiquitin chain. Mol Cell Biol 14(12):7876–7883
24. Pickart CM (1999) Ubiquitin and the stress response. In: Latchman DS (ed) Stress proteins. Springer, Heidelberg, pp 133–152. https://doi.org/10.1007/978-3-642-58259-2_6
25. Hayashi T, Takada K, Matsuda M (1992) Post-transient ischemia increase in ubiquitin conjugates in the early reperfusion. NeuroReport 3(6):519–520
26. Hochrainer K, Jackman K, Anrather J, Iadecola C (2012) Reperfusion rather than ischemia drives the formation of ubiquitin aggregates after middle cerebral artery occlusion. Stroke 43(8):2229–2235. https://doi.org/10.1161/STROKEAHA.112.650416
27. Hu BR, Janelidze S, Ginsberg MD, Busto R, Perez-Pinzon M, Sick TJ, Siesjo BK, Liu CL (2001) Protein aggregation after focal brain ischemia and reperfusion. J Cereb Blood Flow Metab 21(7):865–875
28. Hochrainer K (2018) Protein modifications with ubiquitin as response to cerebral ischemia-reperfusion injury. Transl Stroke Res 9(2):157–173. https://doi.org/10.1007/s12975-017-0567-x
29. Hata R, Maeda K, Hermann D, Mies G, Hossmann KA (2000) Evolution of brain infarction after transient focal cerebral ischemia in mice. J Cereb Blood Flow Metab 20(6):937–946
30. Abramov AY, Scorziello A, Duchen MR (2007) Three distinct mechanisms generate oxygen free radicals in neurons and contribute to cell death during anoxia and reoxygenation. J Neurosci 27(5):1129–1138. https://doi.org/10.1523/JNEUROSCI.4468-06.2007
31. Chan PH (2001) Reactive oxygen radicals in signaling and damage in the ischemic brain. J Cereb Blood Flow Metab 21(1):2–14. https://doi.org/10.1097/00004647-200101000-00002
32. Ge P, Luo Y, Liu CL, Hu B (2007) Protein aggregation and proteasome dysfunction after brain ischemia. Stroke 38(12):3230–3236
33. Keller JN, Huang FF, Zhu H, Yu J, Ho YS, Kindy TS (2000) Oxidative stress-associated impairment of proteasome activity during ischemia-reperfusion injury. J Cereb Blood Flow Metab 20(10):1467–1473
34. Saito A, Hayashi T, Okuno S, Nishi T, Chan PH (2005) Modulation of p53 degradation via MDM2-mediated ubiquitylation and the ubiquitin-proteasome system during reperfusion after stroke: role of oxidative stress. J Cereb Blood Flow Metab 25(2):267–280
35. Asai A, Tanahashi N, Qiu JH, Saito N, Chi S, Kawahara N, Tanaka K, Kirino T (2002) Selective proteasomal dysfunction in the hippocampal CA1 region after transient forebrain ischemia. J Cereb Blood Flow Metab 22(6):705–710
36. Jackman K, Kunz A, Iadecola C (2011) Modeling focal cerebral ischemia in vivo. Methods Mol Biol 793:195–209. https://doi.org/10.1007/978-1-61779-328-8_13
37. Stoppini L, Buchs PA, Muller D (1991) A simple method for organotypic cultures of nervous tissue. J Neurosci Methods 37(2):173–182
38. Kawano T, Anrather J, Zhou P, Park L, Wang G, Frys KA, Kunz A, Cho S, Orio M, Iadecola C (2006) Prostaglandin E2 EP1 receptors: downstream effectors of COX-2 neurotoxicity. Nat Med 12(2):225–229. https://doi.org/10.1038/nm1362
39. Hochrainer K, Jackman K, Benakis C, Anrather J, Iadecola C (2015) SUMO2/3 is associated with ubiquitinated protein aggregates in the mouse neocortex after middle cerebral artery occlusion. J Cereb Blood Flow Metab 35(1):1–5. https://doi.org/10.1038/jcbfm.2014.180
40. Kahl A, Blanco I, Jackman K, Baskar J, Milaganur Mohan H, Rodney-Sandy R, Zhang S, Iadecola C, Hochrainer K (2018) Cerebral ischemia induces the aggregation of proteins linked

to neurodegenerative diseases. Sci Rep 8(1):2701. https://doi.org/10.1038/s41598-018-21063-z
41. Mulder MP, Witting K, Berlin I, Pruneda JN, Wu KP, Chang JG, Merkx R, Bialas J, Groettrup M, Vertegaal AC, Schulman BA, Komander D, Neefjes J, El Oualid F, Ovaa H (2016) A cascading activity-based probe sequentially targets E1–E2-E3 ubiquitin enzymes. Nat Chem Biol 12(7):523–530. https://doi.org/10.1038/nchembio.2084
42. Schindelin J, Arganda-Carreras I, Frise E, Kaynig V, Longair M, Pietzsch T, Preibisch S, Rueden C, Saalfeld S, Schmid B, Tinevez JY, White DJ, Hartenstein V, Eliceiri K, Tomancak P, Cardona A (2012) Fiji: an open-source platform for biological-image analysis. Nat Methods 9(7):676–682. https://doi.org/10.1038/nmeth.2019
43. Dantuma NP, Lindsten K, Glas R, Jellne M, Masucci MG (2000) Short-lived green fluorescent proteins for quantifying ubiquitin/proteasome-dependent proteolysis in living cells. Nat Biotechnol 18(5):538–543. https://doi.org/10.1038/75406
44. Bence NF, Bennett EJ, Kopito RR (2005) Application and analysis of the GFPu family of ubiquitin-proteasome system reporters. Methods Enzymol 399:481–490
45. Altun M, Kramer HB, Willems LI, McDermott JL, Leach CA, Goldenberg SJ, Kumar KG, Konietzny R, Fischer R, Kogan E, Mackeen MM, McGouran J, Khoronenkova SV, Parsons JL, Dianov GL, Nicholson B, Kessler BM (2011) Activity-based chemical proteomics accelerates inhibitor development for deubiquitylating enzymes. Chem Biol 18(11):1401–1412. https://doi.org/10.1016/j.chembiol.2011.08.018
46. Hershko A, Ciechanover A, Heller H, Haas AL, Rose IA (1980) Proposed role of ATP in protein breakdown: conjugation of protein with multiple chains of the polypeptide of ATP-dependent proteolysis. Proc Natl Acad Sci USA 77(4):1783–1786
47. Ungermannova D, Parker SJ, Nasveschuk CG, Chapnick DA, Phillips AJ, Kuchta RD, Liu X (2012) Identification and mechanistic studies of a novel ubiquitin E1 inhibitor. J Biomol Screen 17(4):421–434. https://doi.org/10.1177/1087057111433843
48. Sanderson TH, Reynolds CA, Kumar R, Przyklenk K, Huttemann M (2013) Molecular mechanisms of ischemia-reperfusion injury in brain: pivotal role of the mitochondrial membrane potential in reactive oxygen species generation. Mol Neurobiol 47(1):9–23. https://doi.org/10.1007/s12035-012-8344-z
49. Ramanathan M, Hassanain M, Levitt M, Seth A, Tolman JS, Fried VA, Ingoglia NA (1999) Oxidative stress increases ubiquitin–protein conjugates in synaptosomes. NeuroReport 10(18):3797–3802
50. Lefaki M, Papaevgeniou N, Chondrogianni N (2017) Redox regulation of proteasome function. Redox Biol 13:452–458. https://doi.org/10.1016/j.redox.2017.07.005
51. Iwabuchi M, Sheng H, Thompson JW, Wang L, Dubois LG, Gooden D, Moseley M, Paschen W, Yang W (2014) Characterization of the ubiquitin-modified proteome regulated by transient forebrain ischemia. J Cereb Blood Flow Metab 34(3):425–432. https://doi.org/10.1038/jcbfm.2013.210
52. Meng L, Mohan R, Kwok BH, Elofsson M, Sin N, Crews CM (1999) Epoxomicin, a potent and selective proteasome inhibitor, exhibits in vivo antiinflammatory activity. Proc Natl Acad Sci USA 96(18):10403–10408
53. Ehlers MD (2003) Activity level controls postsynaptic composition and signaling via the ubiquitin-proteasome system. Nat Neurosci 6(3):231–242. https://doi.org/10.1038/nn1013
54. Aiken CT, Kaake RM, Wang X, Huang L (2011) Oxidative stress-mediated regulation of proteasome complexes. Mol Cell Proteom 10(5):R110 006924. https://doi.org/10.1074/mcp.M110.006924
55. Farout L, Mary J, Vinh J, Szweda LI, Friguet B (2006) Inactivation of the proteasome by 4-hydroxy-2-nonenal is site specific and dependant on 20S proteasome subtypes. Arch Biochem Biophys 453(1):135–142. https://doi.org/10.1016/j.abb.2006.02.003
56. Ishii T, Sakurai T, Usami H, Uchida K (2005) Oxidative modification of proteasome: identification of an oxidation-sensitive subunit in 26 S proteasome. Biochemistry 44(42):13893–13901. https://doi.org/10.1021/bi051336u
57. Ekkebus R, van Kasteren SI, Kulathu Y, Scholten A, Berlin I, Geurink PP, de Jong A, Goerdayal S, Neefjes J, Heck AJ, Komander D, Ovaa H (2013) On terminal alkynes that can react with active-site cysteine nucleophiles in proteases. J Am Chem Soc 135(8):2867–2870. https://doi.org/10.1021/ja309802n
58. Hata R, Maeda K, Hermann D, Mies G, Hossmann KA (2000) Dynamics of regional brain metabolism and gene expression after middle cerebral artery occlusion in mice. J Cereb Blood Flow Metab 20(2):306–315
59. Folbergrova J, Zhao Q, Katsura K, Siesjo BK (1995) N-tert-butyl-alpha-phenylnitrone improves recovery of brain energy state in rats following transient focal ischemia. Proc Natl Acad Sci USA 92(11):5057–5061. https://doi.org/10.1073/pnas.92.11.5057
60. Kisselev AF, Goldberg AL (2005) Monitoring activity and inhibition of 26S proteasomes with fluorogenic peptide substrates. Methods Enzymol 398:364–378. https://doi.org/10.1016/S0076-6879(05)98030-0
61. Davies KJ (2001) Degradation of oxidized proteins by the 20S proteasome. Biochimie 83(3–4):301–310
62. Kamikubo T, Hayashi T (1996) Changes in proteasome activity following transient ischemia. Neurochem Int 28(2):209–212
63. Zhang X, Yan H, Yuan Y, Gao J, Shen Z, Cheng Y, Shen Y, Wang RR, Wang X, Hu WW, Wang G, Chen Z (2013) Cerebral ischemia-reperfusion-induced autophagy protects against neuronal injury by mitochondrial clearance. Autophagy 9(9):1321–1333. https://doi.org/10.4161/auto.25132
64. Liu C, Gao Y, Barrett J, Hu B (2010) Autophagy and protein aggregation after brain ischemia. J Neurochem 115(1):68–78
65. Tian F, Deguchi K, Yamashita T, Ohta Y, Morimoto N, Shang J, Zhang X, Liu N, Ikeda Y, Matsuura T, Abe K (2010) In vivo imaging of autophagy in a mouse stroke model. Autophagy 6(8):1107–1114. https://doi.org/10.4161/auto.6.8.13427
66. Liu X, Yamashita T, Shang J, Shi X, Morihara R, Huang Y, Sato K, Takemoto M, Hishikawa N, Ohta Y, Abe K (2018) Molecular switching from ubiquitin-proteasome to autophagy pathways in mice stroke model. J Cereb Blood Flow Metab. https://doi.org/10.1177/0271678X18810617
67. Bond U, Schlesinger MJ (1985) Ubiquitin is a heat shock protein in chicken embryo fibroblasts. Mol Cell Biol 5(5):949–956
68. Kaneko M, Iwase I, Yamasaki Y, Takai T, Wu Y, Kanemoto S, Matsuhisa K, Asada R, Okuma Y, Watanabe T, Imaizumi K, Nomura Y (2016) Genome-wide identification and gene expression profiling of ubiquitin ligases for endoplasmic reticulum protein degradation. Sci Rep 6:30955. https://doi.org/10.1038/srep30955
69. Hu BR, Wieloch T (1993) Stress-induced inhibition of protein synthesis initiation: modulation of initiation factor 2 and guanine nucleotide exchange factor activities following transient cerebral ischemia in the rat. J Neurosci 13(5):1830–1838
70. Mengesdorf T, Proud CG, Mies G, Paschen W (2002) Mechanisms underlying suppression of protein synthesis induced by transient focal cerebral ischemia in mouse brain. Exp Neurol 177(2):538–546
71. Zhang F, Liu CL, Hu BR (2006) Irreversible aggregation of protein synthesis machinery after focal brain ischemia. J Neurochem 98(1):102–112
72. Kulathu Y, Garcia FJ, Mevissen TE, Busch M, Arnaudo N, Carroll KS, Barford D, Komander D (2013) Regulation of A20 and other OTU deubiquitinases by reversible oxidation. Nat Commun 4:1569. https://doi.org/10.1038/ncomms2567
73. Kumar R, Jangir DK, Verma G, Shekhar S, Hanpude P, Kumar S, Kumari R, Singh N, Sarovar Bhavesh N, Ranjan Jana N, Kanti

Maiti T (2017) S-nitrosylation of UCHL1 induces its structural instability and promotes alpha-synuclein aggregation. Sci Rep 7:44558. https://doi.org/10.1038/srep44558
74. Foster MW, Forrester MT, Stamler JS (2009) A protein microarray-based analysis of S-nitrosylation. Proc Natl Acad Sci USA 106(45):18948–18953. https://doi.org/10.1073/pnas.0900729106
75. Komander D, Clague MJ, Urbe S (2009) Breaking the chains: structure and function of the deubiquitinases. Nat Rev Mol Cell Biol 10(8):550–563. https://doi.org/10.1038/nrm2731
76. Lackovic J, Howitt J, Callaway JK, Silke J, Bartlett P, Tan SS (2012) Differential regulation of Nedd4 ubiquitin ligases and their adaptor protein Ndfip1 in a rat model of ischemic stroke. Exp Neurol 235(1):326–335. https://doi.org/10.1016/j.expneurol.2012.02.014
77. Tolbert BS, Tajc SG, Webb H, Snyder J, Nielsen JE, Miller BL, Basavappa R (2005) The active site cysteine of ubiquitin-conjugating enzymes has a significantly elevated pKa: functional implications. Biochemistry 44(50):16385–16391. https://doi.org/10.1021/bi0514459
78. Cheng L, Watt R, Piper PW (1994) Polyubiquitin gene expression contributes to oxidative stress resistance in respiratory yeast (*Saccharomyces cerevisiae*). Mol Gen Genet 243(3):358–362
79. Kim MN, Choi J, Ryu HW (1853) Ryu KY (2015) Disruption of polyubiquitin gene Ubc leads to attenuated resistance against arsenite-induced toxicity in mouse embryonic fibroblasts. Biochim Biophys Acta 5:996–1009. https://doi.org/10.1016/j.bbamcr.2015.02.010
80. Min JW, Lu L, Freeling JL, Martin DS, Wang H (2017) USP14 inhibitor attenuates cerebral ischemia/reperfusion-induced neuronal injury in mice. J Neurochem 140(5):826–833. https://doi.org/10.1111/jnc.13941
81. Liu H, Povysheva N, Rose ME, Mi Z, Banton JS, Li W, Chen F, Reay DP, Barrionuevo G, Zhang F, Graham SH (2019) Role of UCHL1 in axonal injury and functional recovery after cerebral ischemia. Proc Natl Acad Sci USA 116(10):4643–4650. https://doi.org/10.1073/pnas.1821282116
82. Liu H, Li W, Ahmad M, Miller TM, Rose ME, Poloyac SM, Uechi G, Balasubramani M, Hickey RW, Graham SH (2011) Modification of ubiquitin-C-terminal hydrolase-L1 by cyclopentenone prostaglandins exacerbates hypoxic injury. Neurobiol Dis 41(2):318–328. https://doi.org/10.1016/j.nbd.2010.09.020
83. Flick K, Ouni I, Wohlschlegel JA, Capati C, McDonald WH, Yates JR, Kaiser P (2004) Proteolysis-independent regulation of the transcription factor Met4 by a single Lys 48-linked ubiquitin chain. Nat Cell Biol 6(7):634–641. https://doi.org/10.1038/ncb1143
84. Tyrrell A, Flick K, Kleiger G, Zhang H, Deshaies RJ, Kaiser P (2010) Physiologically relevant and portable tandem ubiquitin-binding domain stabilizes polyubiquitylated proteins. Proc Natl Acad Sci USA 107(46):19796–19801. https://doi.org/10.1073/pnas.1010648107